The Effects of Astragalus Polysaccharide on Bone Marrow-Derived Mesenchymal Stem Cell Proliferation and Morphology Induced by A549 Lung Cancer Cells

Authors' Contribution:
Study Design A
Data Collection B
Statistical Analysis C
Data Interpretation D
Manuscript Preparation E
Literature Search F
Funds Collection G

ACD 1 Yue-Mei Zhang*
AFG 2,3 Yong-Qi Liu*
CD 2 Dongling Liu
BC 2 Liying Zhang
AB 1 Jie Qin
AB 2 Zhiming Zhang
AF 2 Yun Su
BD 2 Chunlu Yan
BF 2 Ya-Li Luo
FG 2,3 Jintian Li
AD 4 Xiaodong Xie
AFG 1 Quanlin Guan

1 Department of Oncology, First Hospital of Lanzhou University, Lanzhou, Gansu, P.R. China
2 Provincial-Level Key Laboratory for Molecular Medicine of Major Diseases and The Prevention and Treatment with Traditional Chinese Medicine Research in Gansu Colleges and University, Lanzhou, Gansu, P.R. China
3 Key Laboratory of Dunhuang Medical and Transformation, Ministry of Education of The People's Republic of China, Lanzhou, Gansu, P.R. China
4 Institute of Genetics, School of Basic Medical Sciences, Lanzhou University, Lanzhou, Gansu, P.R. China

Corresponding Author: * Yue-Mei Zhang and Yong-Qi Liu contributed equally to this work
Quanlin Guan, e-mail: guanquanlin116@163.com
Source of support: This work was funded by the National Natural Science Foundation of China (Grant number 81473457 and 81603407)

Background: The tumor microenvironment in lung cancer plays an important role in tumor progression and metastasis. Bone marrow-derived mesenchymal stem cells (MSCs) co-cultured with A549 lung cancer cells show changes in morphology, increase cell proliferation, and cell migration. This study aimed to investigate the effects of Astragalus polysaccharide (APS), a traditional Chinese herbal medicine, on the changes induced in bone marrow-derived MSCs by A549 lung cancer cells *in vitro*.

Material/Methods: Bone marrow-derived MSCs were co-cultured with A549 cells (Co-BMSCs). Co-cultured bone marrow-derived MSCs and A549 cells treated with 50 µg/ml of APS (Co-BMSCs + APS) were compared with untreated Co-BMSCs. Cell proliferation was measured using the cell counting kit-8 (CCK-8) assay. Flow cytometry evaluated the cell cycle. Microarray assays for mRNA expression and Western blot for protein expression were used.

Results: Compared with untreated Co-BMSCs, APS treatment of Co-BMSCs improved cell morphology, reduced cell proliferation, and inhibited cell cycle arrest. The mitogen-activated protein kinase (MAPK)/nuclear factor-kappa B (NF-κB) pathway, TP53, caspase-3, acetylated H4K5, acetylated H4K8, and acetylated H3K9 were involved in the regulatory process.

Conclusions: APS treatment reduced cell proliferation and morphological changes in bone marrow-derived MSCs that were co-cultured with A549 lung cancer cells *in vitro*.

MeSH Keywords: **Adult Stem Cells • Astragalus Plant • Genes, Neoplasm**

Full-text PDF: https://www.medscimonit.com/abstract/index/idArt/914219

📄 3591   🖼 1   📊 6   📚 47

Background

Tumorigenesis depends on intercellular communication and other extracellular signals between tumor and mesenchymal cells and the tumor microenvironment [1]. The tumor microenvironment influences tumor progression and metastasis [2]. The complex milieu of non-malignant cells in the tumor microenvironment contributes to tumor progression by cell-cell interaction [3]. Bone marrow-derived mesenchymal stem cells (MSCs) are progenitor cells that can differentiate into a variety of somatic lineages and contribute to the maintenance and regeneration of several tissues, including bone, adipose tissue, cartilage, and muscle [4].

In the tumor microenvironment, the interaction between bone marrow-derived MSCs and cancer cells remains controversial. MSCs have been reported to play pro-tumorigenic roles and anti-tumorigenic roles [5]. Previous studies have shown that tumors can recruit MSCs into the microenvironment, where they can affect tumor cell survival, angiogenesis, and metastasis [6–8]. Further studies have shown that bone marrow-derived MSCs are capable of delivering anti-tumor agents as a gene therapy vehicle to the tumor sites in certain types of cancer [9,10]. The relationships between MSCs and lung cancer remain to be investigated.

Recent studies have shown the roles of MSCs in the microenvironment in lung cancer. MSCs may promote or inhibit lung cancer cell growth. Some studies have shown that radiation therapy enhances the recruitment of MSCs into the lung cancer microenvironment and is associated with cancer recurrence [11]. MSC-containing microenvironments can have been shown to enhance the activation of autophagy by stimulating epithelial-mesenchymal transition (EMT) and promote migration of A549 lung cells *in vitro* [12]. Also, bone marrow-derived MSCs have been shown to inhibit the proliferation of SK-MES-1 and A549 cells, and induce apoptosis of tumor cells *in vitro* [13].

In 2011, Dai et al. showed that MSCs derived from lung cancer patients had abnormal phenotypes when compared with normal individuals, including increased growth kinetics, reduced expression of TGFβR-I, II, III, PDGFR-α, FGFR-I, EGFR, c-Myc and c-Fos [10]. Lung tumor cell-derived exosomes in the tumor microenvironment induce the pro-inflammatory activity of MSCs, which could support tumor growth [14]. Exosomes derived from A549 cells have been shown to inhibit osteogenic and adipogenic differentiation of adipose tissue-derived MSCs (AD-MSCs), which are involved in changes in long noncoding RNAs (lncRNAs) and mRNAs [15]. How the altered phenotype of MSCs in response to cancer cells and in other diseases impact tumor progression remains poorly understood.

In China, *Astragalus membranaceus*, known as Huang Qi, is one of the most commonly used anti-aging herbs in traditional Chinese medicine (TCM), and has been widely used to treat diseases including diabetes and myocardial infarction [16,17]. Astragalus polysaccharide (APS) is the main active ingredient of *Astragalus membranaceus* and has pro-angiogenic and anti-inflammatory properties as well as protective effects on various organs [18–20]. Recent studies have shown that APS can reduce the proliferation of bone marrow-derived MSCs caused by ferric ammonium citrate-induced iron overload [21]. Treatment with APS also inhibits ionizing radiation-induced bystander effects in bone marrow-derived MSCs [22], has significant antitumor activity in human lung cancer cells [23], and exerts a protective effect on injury due to inflammation [24]. However, the role of APS in bone marrow-derived MSCs induced by lung cancer cells remains to be investigated.

Therefore, this study aimed to investigate the effects of APS, a traditional Chinese herbal medicine, on the changes induced in bone marrow-derived MSCs by A549 lung cancer cells *in vitro*.

Material and Methods

Cell culture and co-culture experiments with bone marrow-derived mesenchymal stem cells (MSCs) and A549 lung cancer cells

Bone marrow-derived mesenchymal stem cells (MSCs) (Cyagen Biosciences Inc, Santa Clara, CA, USA) were cultured in complete medium containing 10% fetal bovine serum (FBS) and Dulbecco's modified Eagle's medium (DMEM/F12) (Hyclone, Logan, UT, USA). The A549 cell line (stored at –80°C) was maintained as a monolayer in RPMI 1640 culture medium (Gibco, Thermo Fisher Scientific, Waltham, MA, USA) containing 10% (v/v) heat-inactivated FBS (Sigma-Aldrich, St. Louis MO, USA), penicillin-streptomycin (Sigma-Aldrich, St. Louis MO, USA), and sodium bicarbonate. Cell aggregates were typically formed after 24 hours incubation at 37°C in a humidified atmosphere with 5% CO_2. Culture medium was replenished every 2–3 days. Cell aggregates were grown in suspension for 3–5 days before they began to attach to the base of the culture bottle. When the cells covered 80–90% of the base of the bottle, they were digested with 0.25% trypsin to perform the co-culture experiments.

A non-contact co-culture system for bone marrow-derived MSCs and A549 lung cancer cells was established by using a transwell insert system. This system consisted of two chambers that were separated by a polyester (PET) film with a pore size of 0.4 μm (Corning, New York, NY, USA). The bone marrow-derived MSCs (5×10^4 cells/chamber) were cultured in the upper chambers, and the A549 cells (1×10^5/well) were cultured

in the bottom of a 6-well plate containing the complete culture medium. The same bone marrow-derived MSCs were cultured in 6-well plates (Corning, New York, NY, USA) containing the complete medium as a control group and cultured at 37°C, in 5% CO_2. The culture medium was replenished every 48 h, and cell growth was observed under an inverted microscope. On the 7th day, cell culture was terminated and single cell suspensions were prepared.

Four groups of cells were studied: A549 cells; untreated bone marrow-derived MSCs as the control group; untreated co-cultured bone marrow-derived MSCs and A549 cells (Co-BMSCs): and co-cultured bone marrow-derived MSCs and A549 cells treated with 50 µg/ml of Astragalus polysaccharide (APS) (Co-BMSCs + APS). APS (purity >98%) was purchased from Shanghai Yuanye Biological Technology Company, China (ZD1219LA13).

Cell morphology and cell cycle assay

The cultured cells were observed every 24 h during culture to examine the changes in cell morphology using an inverted microscope. The harvested cell suspensions were fixed at 4°C in 70% ethanol overnight. Propidium iodide (PI) and RNase A at a final concentration of 50 µg/ml (Beckman Coulter, Inc., Brea, CA, USA) were added to the cells and incubated at 37°C for 30 min. After staining, the cells were washed with PBS. The cellular DNA content was determined using a Cytomics™ FC500 flow cytometer (FCM) (Beckman Coulter, Brea, CA, USA) to analyze the cell cycle, with three replicates per group and three analyses per replication. The results were analyzed graphically using Mod Fit LT software.

Cell counting kit-8 (CCK-8) proliferation assay

APS was dissolved in dimethyl sulfoxide (DMSO) for the co-cultured cell assays. The final culture concentration of DMSO was ≤0.5%. Cell proliferation was analyzed by measuring cell viability with the cell counting kit-8 (CCK-8) assay in each group at different time points. The CCK-8 assay was performed according to the manufacturer's instructions. All cells in the groups were seeded into 96-well plates in triplicate at a density of 2×10^3 cells per well. Cell proliferation was detected at 3 days, 5 days, and 7 days. Then, 20 µl of 10% CCK-8 culture medium was added to the cells at each time point and incubated for 4 h at 37°C. After shaking for 10 min, the absorbance at 450 nm was measured using a Tecan Infinite M200 microplate reader (Tecan, Salzburg, Austria).

Colony forming efficiency assay

Bone marrow-derived MSCs during the exponential growth period were inoculated into a 6-well plate at a density of 100 cells/well, and six replicate wells were used for each group

of cells. After 7 days, the bone marrow-derived MSC colonies were counted. The cultures were fixed with 4% paraformaldehyde for 15 min and stained with crystal violet/methanol (0.005% in 20% methanol) for 10 min. Colony formation was examined under a dissecting microscope. A group of more than 40 contiguous cells was counted as a colony, and the colony-forming efficiency (CFE) was calculated.

Microarray data analysis

Microarray data analysis was performed by Capital Bio Corporation (Beijing, China). Total RNA was prepared using the High Pure RNA Isolation Kit (Roche, Basel, Switzerland) for microarray analysis from three biological replicates of all cell groups. The quality of each RNA sample was assessed using the NanoDrop-1000 (NanoDrop Technologies, Wilmington, DE, USA) and the Agilent 2100 Bioanalyzer (Agilent, Santa Clara, CA, USA). Gene transcription profiles were generated using the Affymetrix GeneChip® Human Gene U133 Plus 2.0 arrays, according to the manufacturer's instructions (Affymetrix, Santa Clara, CA, USA). Microarray data were analyzed using GenomeStudio software version 2011.1 (Illumina, San Diego, CA, USA) and normalized by GenomeStudio Gene Expression Module software version 1.9.0 (Illumina, San Diego, CA, USA). The hierarchical clustering and heatmaps of differentially expressed genes were produced by using Cluster 3.0 software. After clustering, the functional annotations of transcripts were determined by using DAVID Bioinformatics Resources version 6.8 [25,26].

Western blot

The protein expression levels were analyzed using Western blot. The total protein of the cells was extracted using cell lysis buffer (Qiagen, Venlo, the Netherlands), and 30 µg of each protein sample underwent 10% sodium dodecyl sulfate-polyacrylamide gel electrophoresis (SDS-PAGE) with transfer onto polyvinylidene fluoride (PVDF) membranes. The membranes were incubated with blocking buffer containing 5% dried skimmed milk powder and 0.1% Tween 20 (Bio-Rad, Hercules, CA, USA) at 37°C for 3 h, and washed three times with PBST and incubated in blocking buffer. The membranes were incubated in primary antibodies to RAS, P-ERK, NF-κB, P53, and caspase-3 (Abcam, Hong Kong, China) at 4°C overnight. The membranes were then incubated with HRP-conjugated goat anti-rabbit IgG secondary antibodies (Abcam, Hong Kong, China). The membrane staining was quantified using electrochemiluminescence (ECL) for advanced Western blot (Abcam, Hong Kong, China) using a gel imager with β-actin as a reference. The ratio between the target protein and reference protein in the same sample was expressed as the relative expression value of the protein.
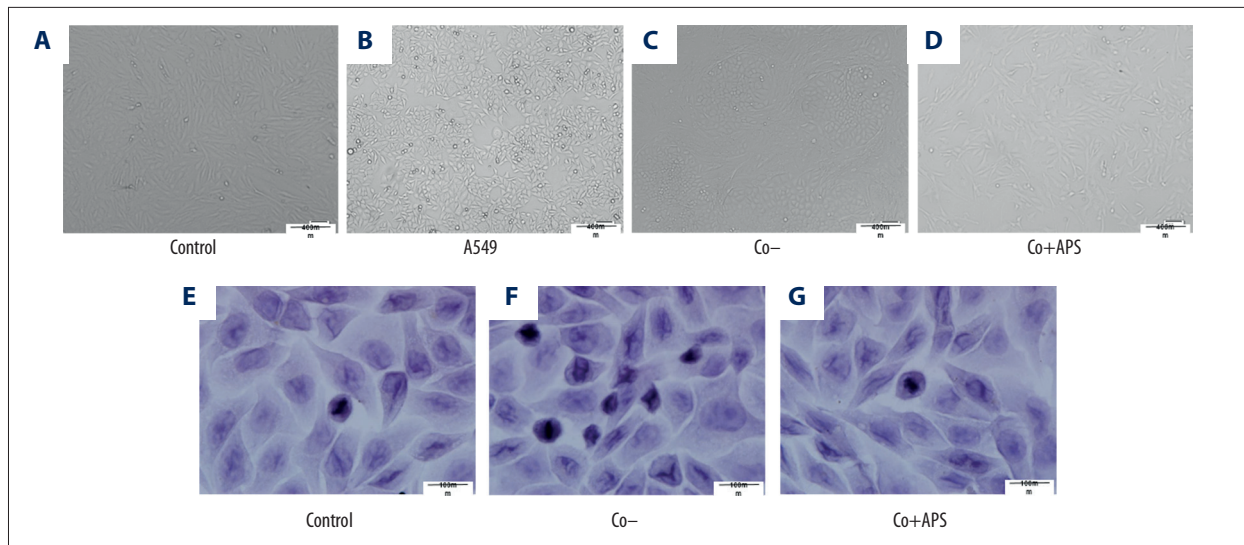
Figure 1. Cell morphology of the A549 lung cancer cells, bone marrow-derived mesenchymal stem cells (MSCs), and bone marrow-derived MSCs co-cultured with A549 cells (Co-BMSCs). (**A**) A549 lung cancer cells show polygonal or fusiform morphology with a lack of cohesion. (**B**) Bone marrow-derived mesenchymal stem cells (MSCs) show fibroblast-like or spindle cell morphology, with a regular arrangement in swirls. (**C**) Bone marrow-derived MSCs co-cultured with A549 cells (Co-BMSCs) grown in culture show short and small, irregularly arranged cells, with irregular polygonal overlapping growth. (**D**) The cells treated with Astragalus polysaccharide (APS), show regular arrangement and are distributed evenly. Magnification, ×100. (**E**) Bone marrow-derived MSCs are spindle-shaped, with regular arrangement. (**F**) Co-BMSCs show enlarged cell nuclei, an irregular nuclear shape, and abnormal mitotic figures. (**G**) APS inhibited the abnormal morphological changes of Co-BMSCs. Hematoxylin staining. Magnification ×1,000.

Statistical analysis

All data were expressed as mean ± standard deviation (SD). The SPSS 17.0 software (SPSS Inc., Chicago, IL, USA) was used to determine statistical significance between groups. One-way analysis of variance (ANOVA) was used to determine the significance the differences between the groups at p<0.05 or p<0.01 level by Tukey's multiple range test.

Results

The effects of treatment with Astragalus polysaccharide (APS) on the morphology of bone marrow-derived mesenchymal stem cells (MSCs)

This *in vitro* study included four groups of cells: A549 lung cancer cells; untreated bone marrow-derived MSCs; untreated bone marrow-derived MSCs co-cultured with A549 cells (Co-BMSCs): and co-cultured bone marrow-derived MSCs and A549 cells treated with 50 µg/ml of APS (Co-BMSCs + APS). The morphology of the untreated control bone marrow-derived mesenchymal stem cells (MSCs) as the control cells were fibroblast-like, spindle-shaped and with adherent growth, with regular cell distribution, clear cell boundaries, and swirl-like growth (Figure 1A).

Following co-culture with bone marrow-derived mesenchymal stem cells (MSCs) cells for 7 days, A549 cells were irregular, polygonal, or fusiform (Figure 1B), Co-BMSCs cells showed abnormal morphology, and were small, disorganized, with irregular polygon overlapping growth (Figure 1C). The morphology of the Co-BMSCs treated with 50 µg/ml of APS, the Co-BMSCs + APS cells, were spindle-shaped, and homogeneous (Figure 1D). Co-BMSCs cells showed enlarged nuclei, with an irregular nuclear shape and density, and visible abnormal mitotic figures and these abnormal morphological changes of the control group and the APS-treated group were not observed (Figure 1E–1G). These results indicated that APS could improve the abnormal cellular morphological features of Co-BMSCs.

The effects of APS on the proliferation of bone marrow-derived MSCs

The CCK-8 assay was used to study the proliferation of the bone marrow-derived MSCs in the cell groups. The data indicated that group Co-BMSCs showed faster growth than the control group, but 50 µg/ml APS could significantly inhibit the proliferation of Co-BMSCs, and had a similar rate of growth to that of the bone marrow-derived MSCs at the 5th and 7th days, compared with the Co-BMSCs (P<0.01) (Figure 2A). The colony-forming count (CFC) of Co-BMSCs treated with 50 µg/ml of APS was significantly lower compared with the Co-BMSCs group (P<0.01), but was there was no significant difference
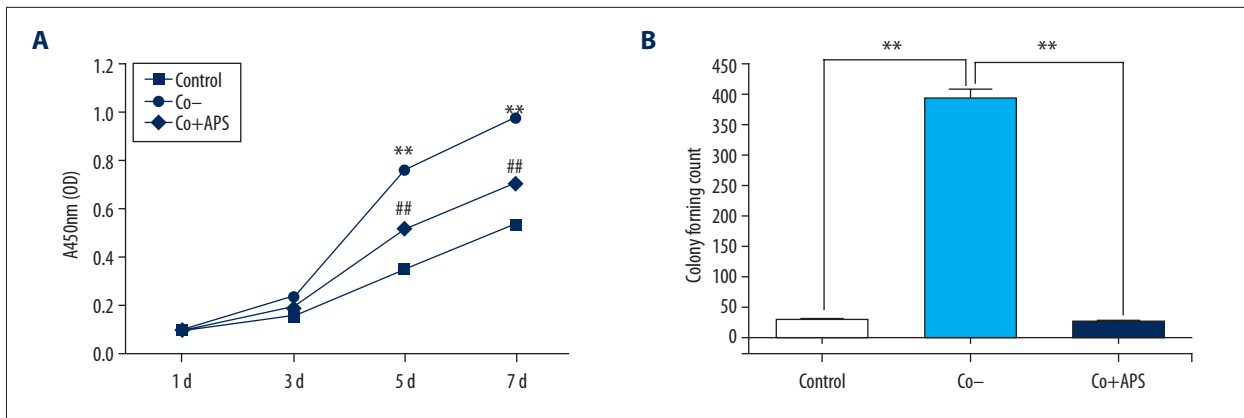
Figure 2. Cell proliferation of the bone marrow-derived mesenchymal stem cells (MSCs) co-cultured with A549 cells (Co-BMSCs) and co-cultured bone marrow-derived MSCs and A549 cells treated with 50 μg/ml of Astragalus polysaccharide (APS) (Co-BMSCs + APS). (**A**) Bone marrow-derived mesenchymal stem cells (MSCs) co-cultured with A549 cells (Co-BMSCs) show increased cell proliferation compared with bone marrow-derived (MSCs). Co-cultured bone marrow-derived MSCs and A549 cells treated with 50 μg/ml of Astragalus polysaccharide (APS) (Co-BMSCs + APS) inhibited the proliferation of Co-BMSCs at 3, 5, and 7 days. (**B**) The colony-forming count of Co-BMSCs treated with 50 μg/ml APS was significantly lower than that in the untreated Co-BMSCs group, but with no significant difference when compared with the bone marrow-derived mesenchymal stem cell (MSC) group. Compared with the bone marrow-derived MSCs, ** p<0.01; Compared with Co-BMSCs, ## p<0.01.
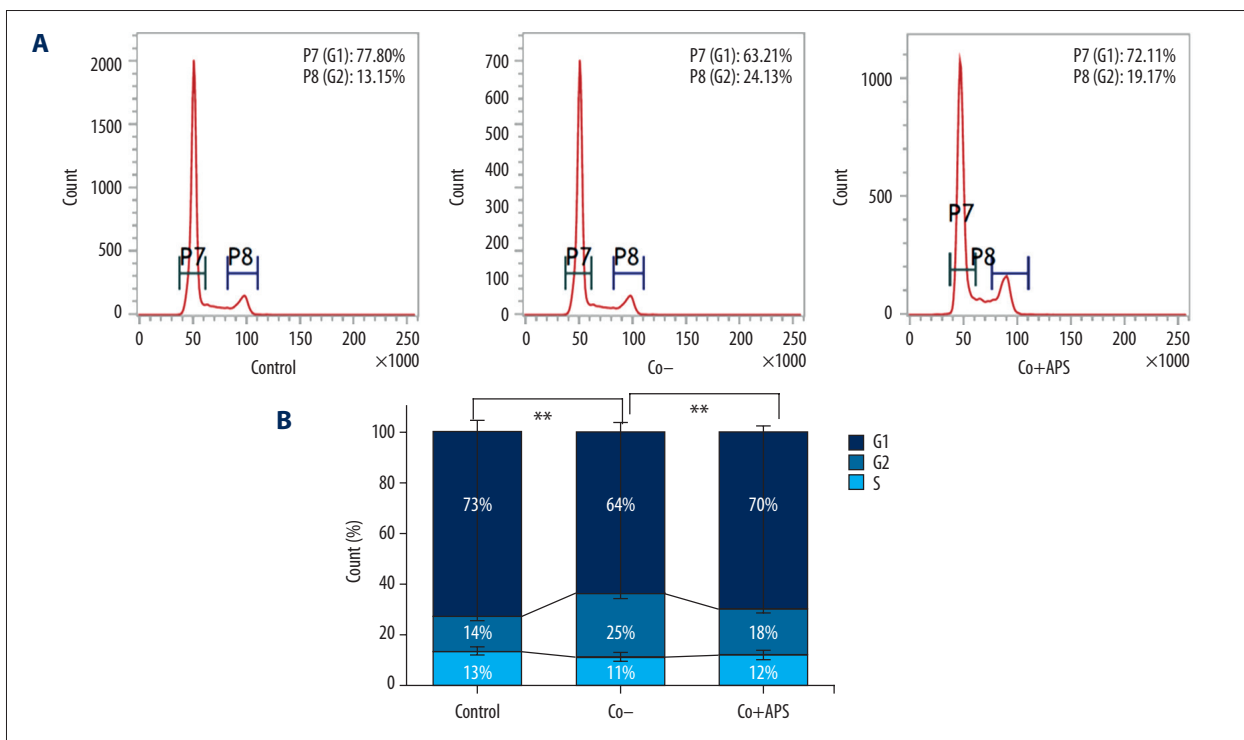
Figure 3. Cell cycle phase analysis using flow cytometry and graphical representation using Mod Fit LT software of the bone marrow-derived mesenchymal stem cells (MSCs), the bone marrow-derived MSCs co-cultured with A549 cells (Co-BMSCs), and the Co-BMSCs treated with 50 μg/ml of Astragalus polysaccharide (APS) (Co-BMSCs + APS). (**A**) The cell cycle analysis of G0/G1-phase, S-phase and G2/M-phase in the bone marrow-derived mesenchymal stem cells (MSCs), the bone marrow-derived MSCs co-cultured with A549 cells (Co-BMSCs), and the Co-BMSCs treated with 50 μg/ml of Astragalus polysaccharide (APS) (Co-BMSCs + APS), respectively. (**B**) The percentage of cells in each phase of the cell cycle in the bone marrow-derived MSCs, the Co-BMSCs, and the co-cultured bone marrow-derived MSCs and A549 cells treated with 50 μg/ml of APS (Co-BMSCs + APS), respectively. The results shown are representative of three independent experiments. Bars with ** p<0.01.

with bone marrow-derived MSC group (P>0.05) (Figure 2B). These results indicated that APS could reduce the proliferation rate of Co-BMSCs.

The effects of APS treatment on the cell cycle

The cell cycle phases in the cultured cell groups were counted using the flow cytometry. Compared with bone marrow-derived MSCs, the number of G1-phase cells in Co-BMSCs group were lower and the number of G2-phase cells was significantly increased (P<0.01). Treatment with 50 µg/ml of APS (the Co-BMSCs + APS group) significantly reduced the effect of Co-BMSCs on the reduction of G1-phase cells and on the increase of G2-phase cells (P<0.01). There was no significant difference in the percentage of cells in the G1-phase and G2-phase between the bone marrow-derived MSCs and Co-BMSCs treated with 50 µg/ml APS (the Co-BMSCs + APS group) (P>0.05). The percentage of bone marrow-derived MSCs were 72.53±4.29% in the G0/G1-phase and 14.15±1.67% in the G2/M-phase. The percentage of cells were 63.57±3.57% in the G0/G1-phase, and 25.13±1.98% in the G2/M-phase in the Co-BMSCs cells. In the Co-BMSCs + APS group, the percentage of cells was 69.87±2.21% in the G0/G1-phase, and 17.97 ± 1.67% in the G2/M-phase (Figure 3A, 3B). There were no significant changes between the cell groups for cells in the S-phase. These results indicated that treatment with 50 µg/ml APS significantly inhibited the effect of Co-BMSCs on cell cycle arrest.

Gene expression in the different groups of bone marrow-derived mesenchymal stem cells (MSCs)

To investigate the difference of transcriptomes between the Co-BMSCs + APS group and the Co-BMSCs group, transcription profiles comprising 31,198 genes were determined with Affymetrix GeneChip® Human Gene U133 Plus 2.0 arrays. There were 3,492 genes (upregulated: 1,858; down-regulated: 1,634) out of 31,198 genes that were differentially expressed (fold change ≥2; P-value ≤0.05) (Figure 4A). The 30 most differentially expressed genes are listed in Table 1. Gene Ontology (GO) analysis of biological process showed that enrichment of the top 10 down-regulated mRNAs mainly participated in several biological processes associated with malignancy, including cell migration, cell motility, and cell adhesion. Enrichment of the top 10 upregulated mRNAs showed that they were involved in the negative regulation of biosynthetic processes and metabolic processes (Figure 4B, 4C). These transcriptional patterns supported that APS could improve the abnormal state of Co-BMSCs.

Protein expression levels

As shown in Figure 5, when compared with the control cells, the protein expression levels of RAS, ERK, NF-PκB p65 in Co-BMSCs were significantly increased (p<0.01), while the expression levels of TP53 and caspase-3 in Co-BMSCs were significantly decreased, and APS significantly reversed these effects (P<0.01). Figure 6 shows that the protein expression level of acetylated H4K5, acetylated H4K8, acetylated H3K9 in Co-BMSCs were significantly increased, while APS markedly reduced the protein expression level of acetylated H4K5, acetylated H4K8, acetylated H3K9 in Co-BMSCs (P<0.01).

Discussion

Worldwide, lung cancer is the leading cause of mortality due to cancer, resulting in 26–28% of all cancer deaths [27]. The lung cancer microenvironment includes stromal cells, growth factors, cytokines and chemokines, which play an important role in the proliferation, survival, migration, and drug resistance of lung cancer [28,29]. Mesenchymal stem cells (MSCs) are the precursors of stromal cells and they can inhibit lung cancer cell proliferation or promote lung cancer growth [30]. Also, MSCs from cancer tissue of lung cancer patients have been shown to accelerate growth kinetics, and reduce sensitivity to cisplatin [30]. MSCs from the bone marrow of lung cancer patients without bone metastasis have shown a low capacity for adipogenic and osteogenic differentiation and increased chondrogenic differentiation [31]. However, the role of the interaction between lung cancer cells and MSCs remains poorly understood.

The present *in vitro* study included four groups of cells, A549 lung cancer cells, untreated bone marrow-derived MSCs, untreated bone marrow-derived MSCs co-cultured with A549 cells (Co-BMSCs), and co-cultured bone marrow-derived MSCs and A549 cells treated with 50 µg/ml of Astragalus polysaccharide (APS) (Co-BMSCs + APS). In a previous study, we reported that Co-BMSCs showed a high rate of proliferation and abnormal changes in morphology, which are findings supported by those of the present study [32]. Previous studies have shown that lung tumor exosomes initiated changes in long non-coding RNA (lncRNA) [15], and induced a pro-inflammatory phenotype of MSCs via the nuclear factor-kappaB (NF-κB) and Toll-like Receptor (TLR) signaling pathways [14]. The findings of the present study showed that the cell proliferation rate and abnormal changes of Co-BMSCs were associated with tumor and inflammation-associated signaling pathways, which require further study.

Astragalus membranaceus has been used as a health food supplement in some Asian populations and has also been used as a medical plant in many herbal formulations to treat a wide variety of diseases. APS is the main compound used in the treatment of inflammatory diseases and cancers and has recently been studied [19,20,23,33]. It has previously been shown that
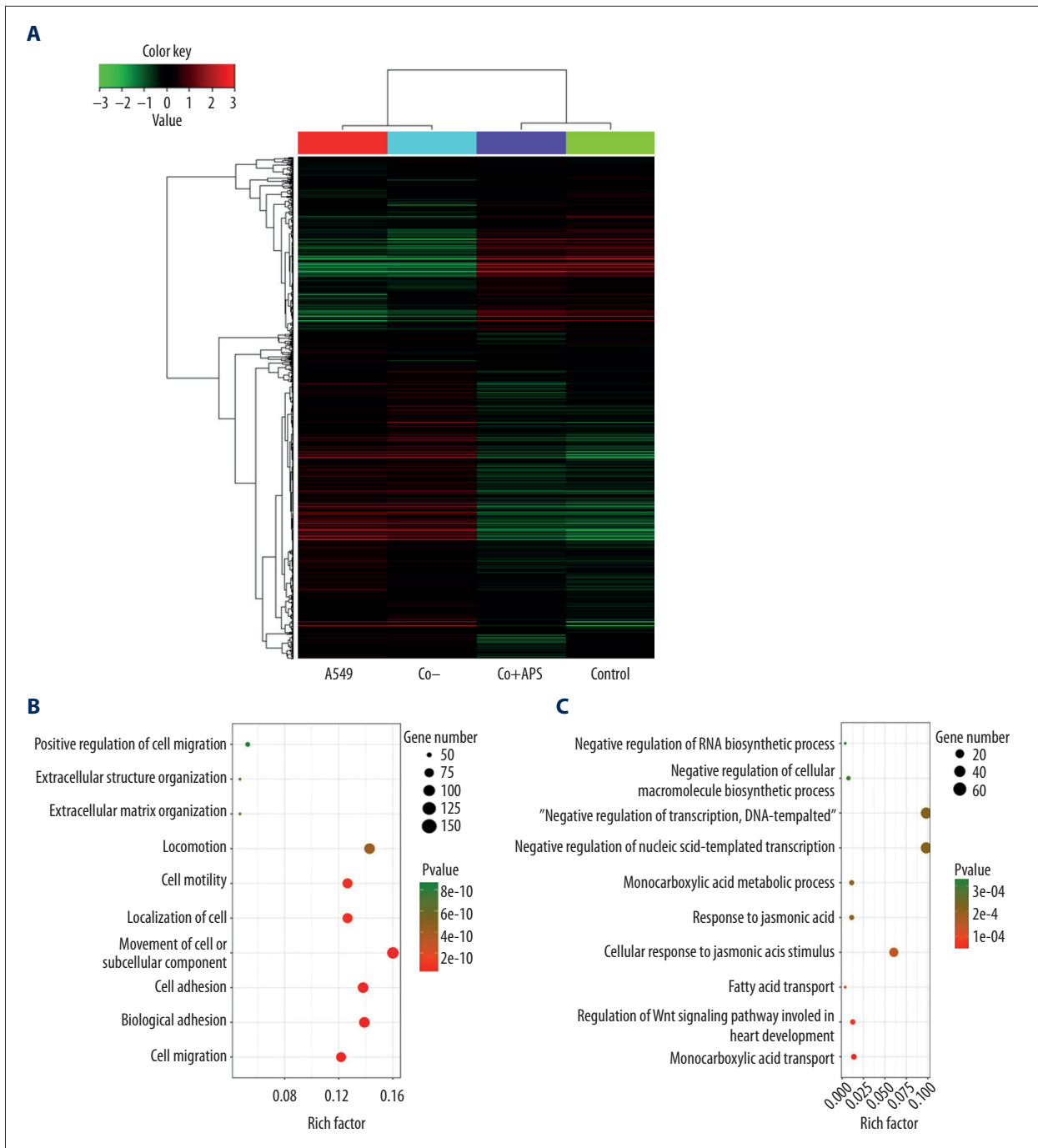
Figure 4. Transcriptional profiling and Gene Ontology (GO) functional analysis of the bone marrow-derived mesenchymal stem cells (MSCs) co-cultured with A549 cells (Co-BMSCs), and co-cultured bone marrow-derived MSCs and A549 cells treated with 50 μg/ml of Astragalus polysaccharide (APS) (Co-BMSCs + APS). (**A**) The heatmap of hierarchical clustering of 3,492 genes that were differentially expressed (fold change >1.5) in Co-BMSCs + APS group compared with the Co-BMSCs group (red, upregulated; green, down-regulated). Functional annotations of down-regulated (**B**) or upregulated (**C**) genes in Co-BMSCs treated with APS compared with the Co-BMSCs. Genes were classified into Gene Ontology (GO) biological process categories using DAVID bioinformatics resources. Bubble plot graphs (**B, C**) were created using OmicShare online analysis.

Table 1. List of the 30 most obviously up-regulated or down-regulated genes by expression microarray.

No.	Gene symbol	Fold change	p-Value	Gene symbol	Fold change	p-Value
1	ALDH3A1	576.64	0.001446	SLC1A3	−526.17	0.003964
2	LGSN	425.07	0.003202	SHISA9	−440.49	0.005271
3	TESC	418.00	0.002281	COL6A3	−397.51	0.000310
4	LINC00473	373.70	0.019420	NDN	−341.70	0.000851
5	SDIM1	349.58	0.005433	MMP3	−317.17	0.000002
6	SLC27A2	322.81	0.023135	NTM	−300.70	0.000319
7	KYNU	277.59	0.008310	COL6A3	−277.97	0.036142
8	ELF3	258.00	0.004790	CCND2	−276.37	0.001281
9	C8orf4	256.25	0.008753	MME	−274.61	0.007626
10	HORMAD1	245.36	0.000045	PDGFRA	−256.25	0.021666
11	MISP	237.91	0.002395	MT1G	−250.28	0.033894
12	LGSN	227.66	0.001510	GALNT15	−210.65	0.008333
13	SCARA5	207.66	0.016869	MME	−203.33	0.008180
14	lnc-SDIM1-3	205.62	0.003704	KRTAP2-3	−200.81	0.004902
15	S100P	197.44	0.013264	lnc-PRICKLE2-3	−199.22	0.000601
16	MNX1	186.42	0.002098	STMN2	−194.36	0.047896
17	ZIC5	173.70	0.002748	LOC101928036	−185.74	0.000022
18	C11orf86	169.37	0.007519	CHRDL1	−181.60	0.003963
19	LLGL2	167.69	0.009801	RAMP1	−178.62	0.000724
20	FGB	167.26	0.046121	LYPD6B	−175.97	0.000190
21	CP	157.70	0.034608	SNHG18	−174.50	0.010205
22	FA2H	146.97	0.023216	FLI1	−164.92	0.003453
23	TM4SF4	146.02	0.023299	SLC37A2	−163.19	0.000961
24	CASC9	145.45	0.000893	SOD3	−162.35	0.035147
25	CCAT1	142.62	0.005465	NEFH	−155.36	0.000195
26	PTPN3	136.20	0.000108	LCP1	−155.22	0.017305
27	INSL4	130.55	0.038424	CDH11	−151.11	0.023628
28	ABCC2	129.34	0.000888	NTNG1	−141.88	0.000469
29	PPP1R9A	123.54	0.005461	WASF3	−140.78	0.000089
30	PTPN3	117.43	0.000539	DAAM2	−140.52	0.027227

APS has significant antitumor activity in human A549 lung cancer cells and NCI-H358 cells [23], and APS inhibited the growth of Lewis lung cancer cells and enhanced the therapeutic effect when combined with cisplatin [34]. APS has been shown to inhibit cell apoptosis, and reduce the proliferation and differentiation of bone marrow-derived MSCs following ferric ammonium citrate-induced iron overload [21]. Zhang et al. reported that APS had protective effects on cell survival level of bystander cells cultured in conditioned medium and maintained the stability of the genome by reducing the number of 53BP1 foci and micronuclei [22]. Current understanding of the effects of APS on bone marrow-derived MSCs in the lung
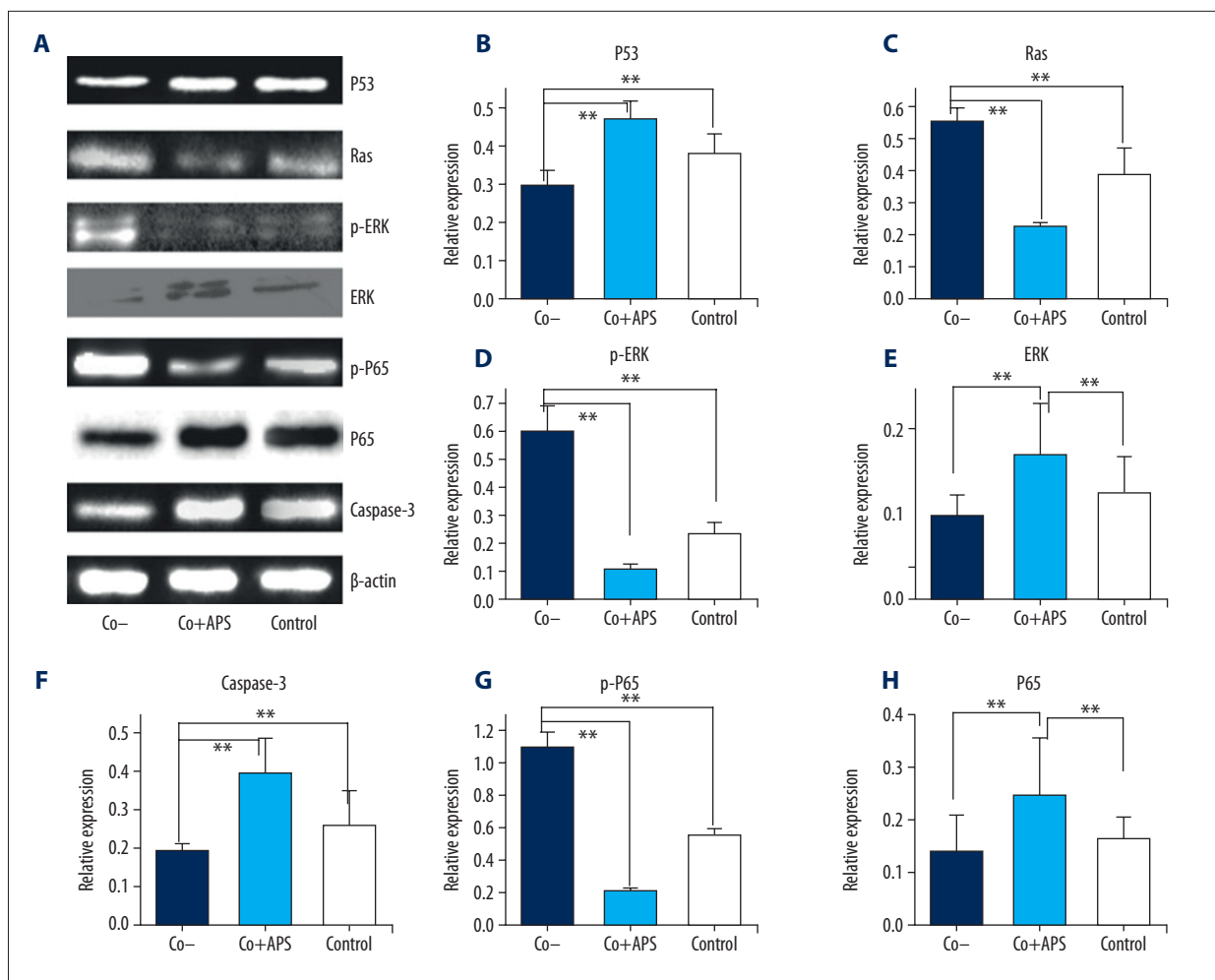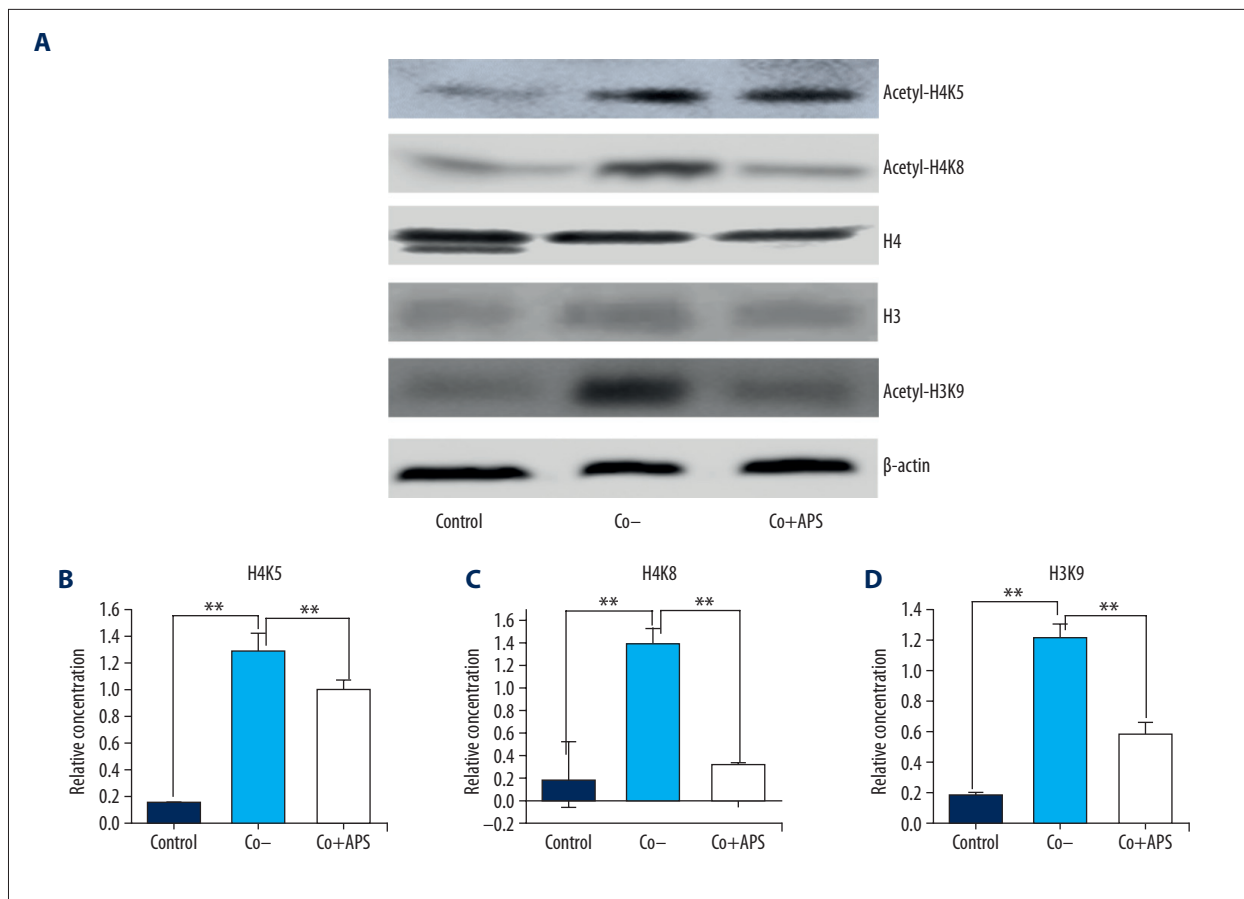
Figure 5. Western blot analysis of protein expression associated with cell proliferation and differentiation signaling pathways. (**A**) The differential protein expression of P53, Ras, P-ERK, NF-κB and caspase-3, in the bone marrow-derived mesenchymal stem cells (MSCs), the bone marrow-derived MSCs co-cultured with A549 cells (Co-BMSCs), and the co-cultured bone marrow-derived MSCs and A549 cells treated with 50 μg/ml of APS (Co-BMSCs + APS). β-actin was used as a loading control. Representative and quantitative Western blot results are shown for P53 (**B**), Ras (**C**), p-ERK (**D**), total ERK (**E**), caspase-3 (**F**), p-P65 (**G**) and total P65 (**H**), respectively. The results are presented as the mean ± standard deviation (SD) of three individual experiments and calculated as relative levels of controls. Bars with ** $p<0.01$.

cancer microenvironment remains unknown. In the present study, the effects of APS on cell morphology, cell proliferation, and cell cycle in bone marrow-derived MSCs co-cultured with A549 cells (Co-BMSCs) showed that APS could improve abnormal cell morphology, reduced cell proliferation, and inhibited the effect of Co-BMSCs on cell cycle arrest.

Nuclear factor-kappa B (NF-κB) is a transcription factor that promotes the transcription of pro-inflammatory and anti-inflammatory genes and has been shown to be involved in cell survival and proliferation [35]. APS suppresses TNFα-induced adhesion molecule expression by blocking NF-κB signaling in human vascular endothelial cells [36]. APS treatment has been shown to inhibit NF-κB signaling and reduce colitis-related

tissue injury in a mouse model [37]. APS has been reported to protect H9c2 cells against lipopolysaccharide-induced inflammatory injury, which may be partially due to the regulation of NF-κB signaling pathways [24]. The findings of the present study showed that APS inhibited the activation of NF-κB in bone marrow-derived MSCs cultured with A549.

The MAPK/ERK pathway plays an important role in cell proliferation. APS has been shown to increase the antitumor effects of apatinib by downregulating the phosphorylation of ERK [38]. The findings of the present study also showed that APS reduced RAS/ERK signaling in Co-BMSCs. APS reduced A549-induced tumorigenesis via MAPK/NF-κB signaling pathway in bone marrow-derived MSCs, which are consistent with

Figure 6. Western blot analysis of the protein expression including the acetylated histones in the bone marrow-derived mesenchymal stem cells (MSCs), bone marrow-derived MSCs co-cultured with A549 cells (Co-BMSCs), and the co-cultured bone marrow-derived MSCs and A549 cells treated with 50 μg/ml of APS (Co-BMSCs + APS). (**A**) Shows the histone of H3, H4 and acetylated histone of H4K5, H4K8, and H3K9 in bone marrow-derived mesenchymal stem cells (MSCs) alone, bone marrow-derived MSCs co-cultured with A549 cells (Co-BMSCs), and the co-cultured bone marrow-derived MSCs and A549 cells treated with 50 μg/ml of APS (Co-BMSCs + APS). β-actin was used as a loading control. Representative and quantitative Western blot results are shown for acetylated H4K5 (**B**), acetylated H4K8 (**C**), acetylated H3K9 (**D**), respectively. Results are presented as the mean ± standard deviation (SD) of three individual experiments and calculated as relative levels compared with the controls. Bars with ** $p < 0.01$.

previous findings that showed that APS inhibited ionizing radiation-induced bystander effects by regulating MAPK/NF-κB signaling pathway in bone marrow-derived MSCs [24]. The results of the present study also showed that APS reduced RAS and ERK protein expression levels in Co-BMSCs, decreased cell proliferation and abnormal morphological changes of Co-BMSCs via the MAPK/NF-κB signaling pathway.

The apoptosis signaling pathway is important for cell proliferation and tumor growth and is mediated by caspases, including caspase-3. Previous studies have shown that APS protected human cardiac microvascular endothelial cells from hypoxia-reperfusion injury by inhibiting the activity of caspase-3 [39]. APS enhanced the anti-proliferative and apoptotic effect of cisplatin by modulating expression of caspases in nasopharyngeal carcinoma cells *in vitro* [33]. The present study showed

that the expression level of caspase-3 in Co-BMSCs was increased, which could be reversed by treatment with APS. Also, p53 is a tumor suppressor, and when its function is lost, tumorigenesis and cancer progression is induced [40,41]. The present study showed that the expression levels of p53 protein of bone marrow-derived MSCs were upregulated by co-culture with A549 cells, and APS suppressed these effects. Previous studies have shown that p53 and Ras contributed to different signal transduction pathways [42]. Inactivation of p53 and activation of Ras can induce the expression of the NF-κB gene, and NF-κB is regulated by p53 and Ras in carcinogenesis [43,44]. The findings of the present study showed that the MAPK/NF-κB pathway, TP53, and caspase-3 were involved in the regulatory effects of APS on improving cellular function in Co-BMSCs, indicating the involvement of multiple signaling pathways in the effects of APS.

Histone acetylation is one of the most frequent post-translational modifications that can regulate chromatin dynamics and the accessibility of DNA in eukaryotes [45]. Altered genome-wide acetylation levels have been found in cancer, including lung cancer, and histone H3 and/or H4 acetylation is associated with lung cancer, including H3K9 and N-α-terminal of histone H4 [46,47]. The findings of the present study showed that, following treatment with APS, the expression levels of H4K5, H4K8, and H3K9 acetylation in Co-BMSCs were significantly increased, and the protein expression level of H4K5, H4K8, and H3K9 acetylation were significantly reduced in Co-BMSCs. These findings suggest that APS may have an epigenetic effect on the microenvironment in malignancy.

Conclusions

An *in vitro* study that included four groups of cells, A549 lung cancer cells, untreated bone marrow-derived MSCs, untreated bone marrow-derived MSCs co-cultured with A549 cells (Co-BMSCs), and co-cultured bone marrow-derived MSCs and A549 cells treated with 50 μg/ml of Astragalus polysaccharide (APS) (Co-BMSCs + APS). The results showed that APS could reverse the abnormal morphological changes, increased cell proliferation, and cell cycle arrest that developed in Co-BMSCs. These effects were regulated by the mitogen-activated protein kinase (MAPK)/nuclear factor-kappa B (NF-κB) pathway, TP53, caspase-3, acetylated H4K5, acetylated H4K8, and acetylated H3K9. Treatment with APS resulted in a protective effect on cell proliferation and morphological changes in bone marrow-derived MSCs induced by A549 lung cancer cells *in vitro*.

Conflict of interest

None.

References:

1. Hanahan D, Weinberg RA: Hallmarks of cancer: The next generation. Cell, 2011; 144: 646–74

2. Rowley DR: Reprogramming the tumor stroma: A new paradigm. Cancer Cell, 2014; 26: 451–52

3. Turley SJ, Cremasco V, Astarita JL: Immunological hallmarks of stromal cells in the tumour microenvironment. Nat Rev Immunol, 2015; 15: 669–82

4. Pittenger MF, Mackay AM, Beck SC et al: Multilineage potential of adult human mesenchymal stem cells. Science, 1999; 284: 143–47

5. Honga IS, Lee HY, Kang KS: Mesenchymal stem cells and cancer: Friends or enemies? Mutat Res, 2014; 768: 98–106

6. Zhu W, Xu W, Jiang R et al: Mesenchymal stem cells derived from bone marrow favor tumor cell growth *in vivo*. Exp Mol Pathol, 2006; 8: 267–74

7. Karnoub AE, Dash AB, Vo AP et al: Mesenchymal stem cells within tumour stroma promote breast cancer metastasis. Nature, 2007; 449: 557–63

8. Beate H, Douaa D, Salita E et al: Role of mesenchymal stem cell-derived fibbrinolytic factor in tissue regeneration and cancer progression. Cell Mol Life Sci, 2015; 72: 4759–70

9. Maestroni GJ, Hertens E, Galli P: Factors from nonmacrophage bone marrow stromal cells inhibit Lewis lung carcinoma and B16 melanoma growth in mice. Cell Mol Life Sci, 1999; 55: 663–67

10. Dai LJ, Moniri MR, Zeng ZR et al: Potential implications of mesenchymal stem cells in cancer therapy. Cancer Lett, 2011; 305: 8–20

11. Wang HH, Cui YL, Zaorsky NG et al: Mesenchymal stem cells generate pericytes to promote tumor recurrence via vasculogenesis after stereotactic body radiation therapy. Cancer Lett, 2016; 375: 349–59

12. Luo D, Hu S, Tang C et al: Mesenchymal stem cells promote cell invasion and migration and autophagy-induced epithelial-mesenchymal transition in A549 lung adenocarcinoma cells. Cell Biochem Funct, 2018; 36: 88–94

13. Li L, Tian H, Chen Z et al: Inhibition of lung cancer cell proliferation mediated by human mesenchymal stem cells. Acta Biochim Biophys Sin, 2011; 43: 143–48

14. Li XX, Wang SH, Zhu RJ et al: Lung tumor exosomes induce a pro-inflammatory phenotype in mesenchymal stem cells via NFκB-TLR signaling pathway. J Hematol Oncol, 2016; 9: 42

15. Wang S, Li XX, Zhu RJ et al: Lung cancer exosomes initiate global long non-coding RNA changes in mesenchymal stem cells. Int J Oncol, 2016; 48: 681–89

16. Chen W, Li YM, Yu MH: Astragalus polysaccharides inhibited diabetic cardiomyopathy in hamsters depending on suppression of heart chymase activation. J Diabetes Complications, 2010; 24: 199–208

17. Liu P, Zhao H, Luo Y: Anti-aging implications of *Astragalus membranaceus* (Huangqi): A well-known Chinese tonic. Aging Dis, 2017; 8: 868–86

18. Yao C, Gao F, Chen Y et al [Experimental research of Astragalus polysaccharides collagen sponge in enhancing angiogenesis and collagen synthesis.] Zhongguo Xiu Fu Chong Jian Wai Ke Za Zhi, 2011; 25: 1481–85 [in Chinese]

19. Lu J, Chen X, Zhang Y et al: Astragalus polysaccharide induces anti-inflammatory effects dependent on AMPK activity in palmitate-treated RAW264.7 cells. Int J Mol Med, 2013; 31: 1463–70

20. Auyeung K, Han Q, Ko J: *Astragalus membranaceus*: A review of its protection against inflammation and gastrointestinal cancers. Am J Chin Med, 2016, 44: 1–22

21. Yang F, Yan G, Li Y et al: Astragalus polysaccharide attenuated iron overload-induced dysfunction of mesenchymal stem cells via suppressing mitochondrial ROS. Cell Physiol Biochem, 2016; 39: 1369–79

22. Zhang L, Luo Y, Lu Z et al: Astragalus polysaccharide inhibits ionizing radiation-induced bystander effects by regulating MAPK/NF-κB signaling pathway in bone mesenchymal stem cells (BMSCs). Med Sci Monit, 2018; 24: 4649–58

23. Wu CY, Ke Y, Zeng YF et al: Anticancer activity of Astragalus polysaccharide in human non-small cell lung cancer cells. Cancer Cell Int, 2017; 17: 115

24. Ren Q, Zhao S, Ren C et al: Astragalus polysaccharide alleviates LPS-induced inflammation injury by regulating miR-127 in H9c2 cardiomyoblasts. Int J Immunopathol Pharmacol, 2018; 32: 1–11

25. Huang W, Sherman B, Lempicki R: Systematic and integrative analysis of large gene lists using DAVID bioinformatics resources. Nat Protoc, 2009; 4: 44–57

26. Huang W, Sherman BT, Lempicki RA: Bioinformatics enrichment tools: Paths toward the comprehensive functional analysis of large gene lists. Nucleic Acids Res, 2009; 37: 1–13

27. Siegel R, Ma J, Zou Z et al: Cancer statistics. Cancer J. Clin, 2014; 64: 9–29

28. Pietras K, Ostman A: Hallmarks of cancer: Interactions with the tumor stroma. Exp Cell Res, 2010; 316: 1324–31

29. Nefertiti E, Leyre L, Werner S et al: Tumor-stromal interactions in lung cancer: Novel candidate targets for therapeutic intervention. Expert Opin Investig Drugs, 2012; 21: 1107–22

30. Gottschling S, Granzow M, Kuner R et al: Mesenchymal stem cells in non-small cell lung cancer – different from others? Insights from comparative molecular and functional analyses. Lung Cancer, 2013; 80: 19–29

31. Fernandez V, Hofer E, Choi H et al: Behaviour of mesenchymal stem cells from bone marrow of untreated advanced breast and lung cancer patients without bone osteolytic metastasis. Clin Exp Metastasis, 2013; 30: 317–32

32. Zhang YM, Zhang ZM, Guan QL et al: Co-culture with lung cancer A549 cells promotes the proliferation and migration of mesenchymal stem cells derived from bone marrow. Exp Ther Med, 2017; 14: 2983–91

33. Zhou Z, Meng M, Ni H: Chemosensitizing effect of Astragalus polysaccharides on nasopharyngeal carcinoma cells by inducing apoptosis and modulating expression of Bax/Bcl-2 ratio and caspases. Med Sci Monit, 2017; 23: 462–69

34. Ming H, Chen Y, Zhang F et al: [Astragalus polysaccharides combined with cisplatin decreases the serum levels of CD44 and collagen type IV and hyaluronic acid in mice bearing Lewis lung cancer.] Xi Bao Yu Fen Zi Mian Yi Xue Za Zhi, 2015; 31: 909–13 [in Chinese]

35. Lawrence T, Bebien M, Liu GY et al: IKKalpha limits macrophage NF-kappaB activation and contributes to the resolution of inflammation. Nature, 2005; 434: 1138–43

36. Zhu YP, Shen T, Lin YJ et al: Astragalus polysaccharides suppress ICAM-1 and VCAM-1 expression in TNF-α-treated human vascular endothelial cells by blocking NF-κB activation. Acta Pharmacol Sin, 2013; 34: 1–7

37. Lv J, Zhang Y, Tian Z et al: Astragalus polysaccharides protect against dextran sulfate sodium-induced colitis by inhibiting NF-κB activation. Int J Biol Macromol, 2017; 98: 723–29

38. Wu J, Wang J, Su Q et al: Traditional Chinese medicine Astragalus polysaccharide enhanced antitumor effects of the angiogenesis inhibitor apatinib in pancreatic cancer cells on proliferation, invasiveness, and apoptosis. Onco Targets Ther, 2018; 11: 2685–98

39. Xie L, Wu Y, Fan Z et al: Astragalus polysaccharide protects human cardiac microvascular endothelial cells from hypoxia/reoxygenation injury: The role of PI3K/AKT, Bax/Bcl-2, and caspase-3. Mol Med Rep, 2016; 14: 904–10

40. Das S, Raj L, Zhao B et al: Hzf, a key modulator of p53 mediated transcription, functions as a critical determinant of cell survival and death upon genotoxic stress. Cell, 2007; 130: 624–37

41. Lukin DJ, Carvajal LA, Liu WJ et al: p53 Promotes cell survival due to the reversibility of its cell-cycle check-points. Mol Cancer Res, 2015; 13: 16–28

42. El-Serafi MM, Bahnassy AA, Ali NM et al: The prognostic value of c-Kit, K-ras codon 12, and p53 codon 72 mutations in Egyptian patients with stage II colorectal cancer. Cancer, 2010; 116: 4954–64

43. Enomoto T, Fujita M, Inoue M et al: Alterations of the p53 tumor suppressor gene and its association with activation of the c-K-ras-2 protooncogene in premalignant and malignant lesions of the human uterine endometrium. Cancer Res, 1993; 53: 1883–88

44. Buganim Y, Solomon H, Rais Y et al: p53 Regulates the Ras circuit to inhibit the expression of a cancer-related gene signature by various molecular pathways. Cancer Res, 2010; 70: 2274–84

45. Strahl BD, Allis CD: The language of covalent histone modifications. Nature, 2000; 403: 41–45

46. Barlési F, Giaccone G, Gallegos-Ruiz MI et al: Global histone modifications predict prognosis of resected non small-cell lung cancer. J Clin Oncol. 2007; 25: 4358–64

47. Ju J, Chen A, Deng Y et al: NatD promotes lung cancer progression by preventing histone H4 serine phosphorylation to activate Slug expression. Nat Commun, 2017; 8: 928

This work is licensed under Creative Common Attribution-NonCommercial-NoDerivatives 4.0 International (CC BY-NC-ND 4.0)

4121

Indexed in: [Current Contents/Clinical Medicine] [SCI Expanded] [ISI Alerting System] [ISI Journals Master List] [Index Medicus/MEDLINE] [EMBASE/Excerpta Medica] [Chemical Abstracts/CAS]